On the Evolutionary Status of the Early–type Galaxy Population in Abell 2390

Alexander Fritz[1]*, Bodo L. Ziegler[1], Richard G. Bower[2], Ian Smail[2], Roger L. Davies[3]

[1]Universitäts–Sternwarte Göttingen, Geismarlandstraße 11,
D-37083 Göttingen, Germany
[2]Department of Physics, University of Durham, Durham DH1 3LE, UK
[3]University of Oxford, Astrophysics, Keble Road, Oxford OX1 3RH, UK

June 27, 2003

Abstract

Using a combination of Multi-Object-Spectroscopy (MOS) with MOSCA at the 3.5 m telescope on Calar Alto Observatory, deep ground-based imaging with the 5.1 m Hale telescope at Palomar Observatory and *HST* observations in the F555W (B) and F814W (I) filters, a large sample of $N = 51$ early-type galaxies in the rich cluster Abell 2390 at a redshift $z = 0.23$ is investigated. Our study spans both a broad range in luminosity ($-19.3 \geq M_B \geq -22.3$) and a wide field-of-view ($10' \times 10'$). Therefore, the environmental dependence of different formation scenarios can be analysed in detail as a function of radius from the cluster centre as well as for different sub-populations.

In this article we present the motivation for this investigation, give an overview of the sample selection and observations and present our findings for the Fundamental Plane of early-type galaxies for the intermediate redshift clusters Abell 2218 and Abell 2390 at $z \sim 0.2$.

1 Introduction

One of the key questions of early-type galaxy evolution is when and within what timescales their stellar populations have been formed. Although numerous studies on early-type galaxies in the local universe have been performed (e.g., Dressler et al. 1987; Bender, Burstein & Faber 1992; 1993) to address this question, there are still two competing formation scenarios, the monolithic collapse model and the paradigm of hierachical clustering. On the one hand, theoretical models of a monolithic collapse predict an intense burst of star formation at high redshift ($z_{\rm f} \gtrsim 2$) and a subsequent following passive evolution of the stellar populations. On the other hand, the picture of hierachical galaxy formation (the so-called "bottom-up universe") presumes longer assembly timescales for the more massive galaxies, where galaxy clusters are the result of the highest peaks of primordial density fluctuations and merging of galaxies and the infall of new cold gas from a galaxy's halo being the main drivers. Therefore, galaxies formed through accumulation of small structures result in somewhat younger mean ages.

*E-mail: afritz@uni-sw.gwdg.de

In order to probe the evolution of galaxies, it is necessary to explore both the morphological evolution as well as the evolution of the luminosities and the mass-to-light (M/L) ratios of the galaxies. One of the most powerful tools is the Fundamental Plane of early-type galaxies.

1.1 The Fundamental Plane

In a three dimensional parameter space, defined by three observables, the effective radius $R_{\rm e}$, effective surface brightness $\mu_{\rm e}$ and velocity dispersion σ, the Fundamental Plane (FP) establishes a tight correlation (Dressler et al. 1987, Djorgovski & Davis 1987) in the following form:

$$\log R_e = \alpha \log \sigma + \beta \mu_e + \gamma, \quad (1)$$

where R_e is in units of kpc, σ in km s^{-1}and $\mu_{\rm e}$ in mag/arcsec^2. This empirical relationship relates galaxy structure (the effective radius R_e and the effective surface brightness within R_e, μ_e) to kinematics (velocity dispersion σ).
Elliptical galaxies do not fill this FP plane entirely, but rather are restricted to a certain band within it (Guzmán, Lucey & Bower 1993). Different factors account for the precise form of the FP, known as the lack of exact homology of early-type galaxies, e.g. visible in differences in the luminosity profiles or in the dynamical structure (Caon et al. 1993; Graham et al. 1996). The formation and evolution of early-type galaxies are tightly constraint through the existence of the local FP and its small scatter of ~ 0.1 dex. (see e.g., Bender, Burstein & Faber 1992). Although the FP scatter is small, it is about twice than expected from the measurement errors alone (Jørgensen et al. 1996).
Projections of the FP plane are the the Faber-Jackson relation, luminosity L *vs.* σ relation, (Faber & Jackson 1976) and the Kormendy relation, a correlation between $\mu_{\rm e}$ *vs.* $R_{\rm e}$ (Kormendy 1977), which is the projection of the FP on the photometric plane.

2 Motivation

Cluster environments provide the opportunity to observe a larger number of early-type galaxies with less amount of observing time. However, most previous spectroscopic studies have targetted only a modest number of typically the more luminous (and hence massive) galaxies in each cluster. To overcome possible selection effects and limitations due to a small number of the more luminous galaxies of previous spectroscopic samples, we focus in this investigation of the cluster Abell 2390 on a large number of objects ($N = 51$), spanning a wide range in luminosity $23.3 > B > 21.4$, corresponding to $-19.2 > M_B > -22.4$ and a wide field of view of $\sim 10' \times 10'$ (2.5×2.5 Mpc), analogous to the study of Abell 2218 by Ziegler et al. (2001). Furthermore, the evolution of galaxies in age, metallicity and abundance ratios is explored by analysing absorption line strengths (e.g., Balmer lines, $\rm CN_1$, $\rm Mg_b$, Fe-indices), and comparing them with recent stellar population models (SSP) by Thomas et al. (2003) using (α–Fe) enhancements. The large data set makes it feasible to study possible evolution of the slope and zeropoint of the Mg$-\sigma$ and Faber-Jackson relations. Thus, with this large sample, it is possible to explore variations in early-type galaxy evolution not only in the dense core of a rich cluster but also in the less dense environment in the outskirts of a cluster by incorporating galaxies at larger radii from the cluster centre.

3 Sample Selection, Observations and Data Reduction

The large spectroscopic sample of this investigation comprises a total of 63 spectra of 51 different early-type galaxies gained using the MOSCA spectrograph at the 3.5 m telescope at Calar Alto Observatory in Spain during two observing runs (September 1999 and July 2000). The spectral resolution in the wavelength range $5900 \lesssim \lambda \lesssim 6400$ Å (around the $H\beta$ and Mg_b lines) was 5.5 Å FWHM, corresponding to $\sigma_{\mathrm{inst}} \sim 100$ km s^{-1}. Values for the S/N vary between 9.6 and 79.8 with an average value of $S/N \sim 41$.

The objects were selected using ground-based Gunn i-band images (500 sec) obtained with the Palomar 5 m Hale telescope. In particular, in the selection procedure for the mask design special care was taken that galaxies cover the whole field-of-view (FOV) of MOSCA (see Fig. 1), to accomplish one of our main aims to study the environmental dependence of the evolution of elliptical galaxies. Additional imaging data from Mt. Palomar is available in the U (3000 sec) and B (500 sec) filter bands and A 2390 was also observed with the WFPC2 camera onboard the *Hubble Space Telescope (HST)* in theF555W and F814W filter (10800 sec each).

All spectra were reduced using standard reduction techniques implemented within MIDAS and IRAF. Examples of final 1-dimensional spectra in rest frame wavelengths are plotted in Fig. 2. The velocity dispersions were derived with the Fourier Correlation Quotient method as introduced by Bender (1990).

Absolute magnitudes for all galaxies were calculated from our ground-based UBi photometry. Using SExtractor (Bertin & Arnouts 1996), object positions were determined and performing aperture photometry apparent magnitudes were measured. Gunn i magnitudes were transformed to rest frame B and rest frame Gunn r magnitudes with typical k-corrections of $k_B \approx 1.2$ and $k_r \approx 0.34$, for HST objects according to their morphology. A more detailed description on the data reduction and analysis procedures can be found in Fritz et al. (2003b).

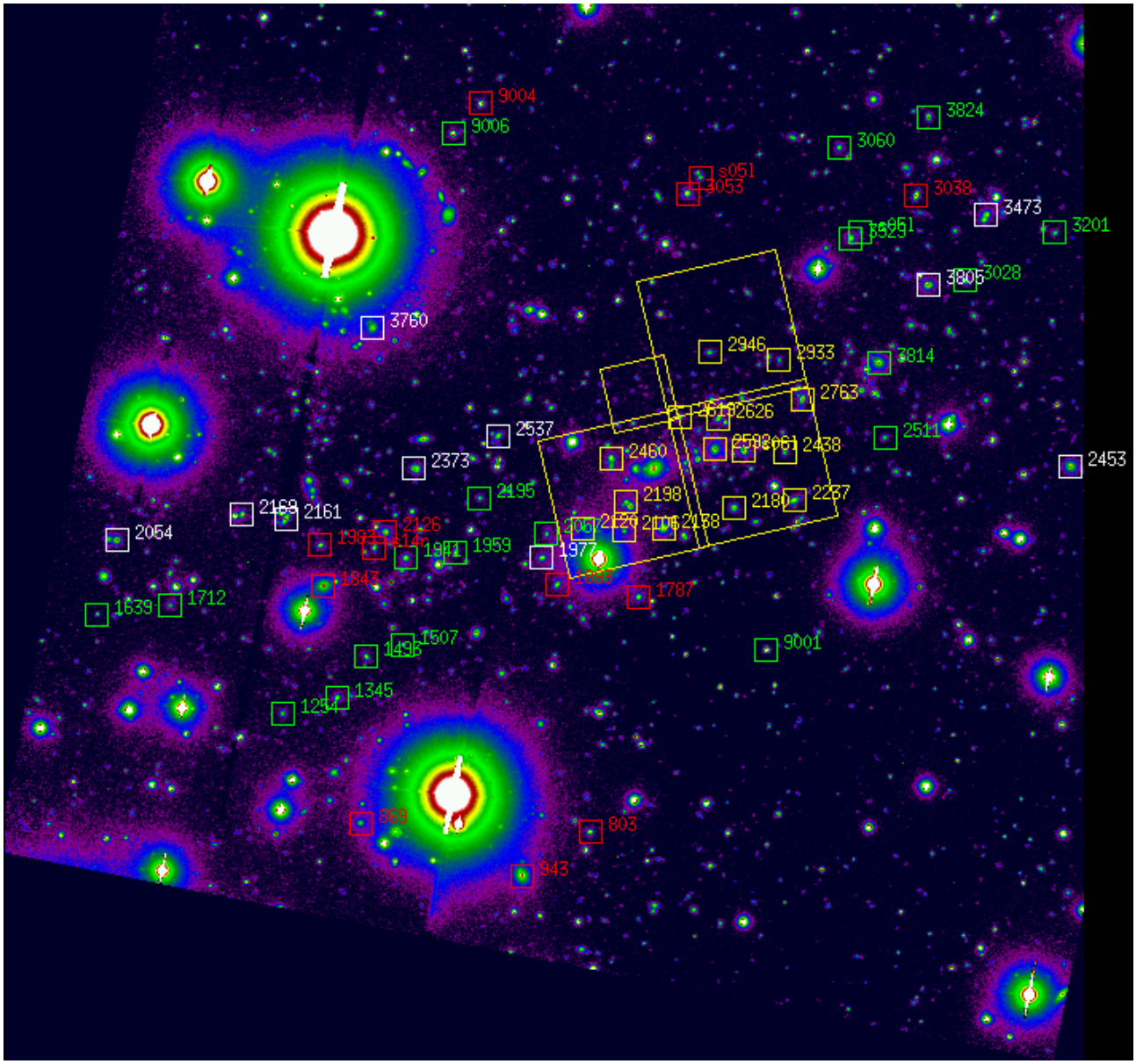

Figure 1: Hale Gunn i image of the cluster A 2390 at $z = 0.23$ taken with the 5.1 m Hale telescope on Mt. Palomar. The total FOV is $11\farcm3 \times 11\farcm4$. North is up, east to the left. The three masks with member galaxies from spectroscopy are shown; mask 1 (white), mask 2 (red), mask 3 (green). Stars used for the mask alignment are labeled as ID = 900x. In yellow an overlay of the HST WFPC2 FOV with those objects falling into this field is indicated.

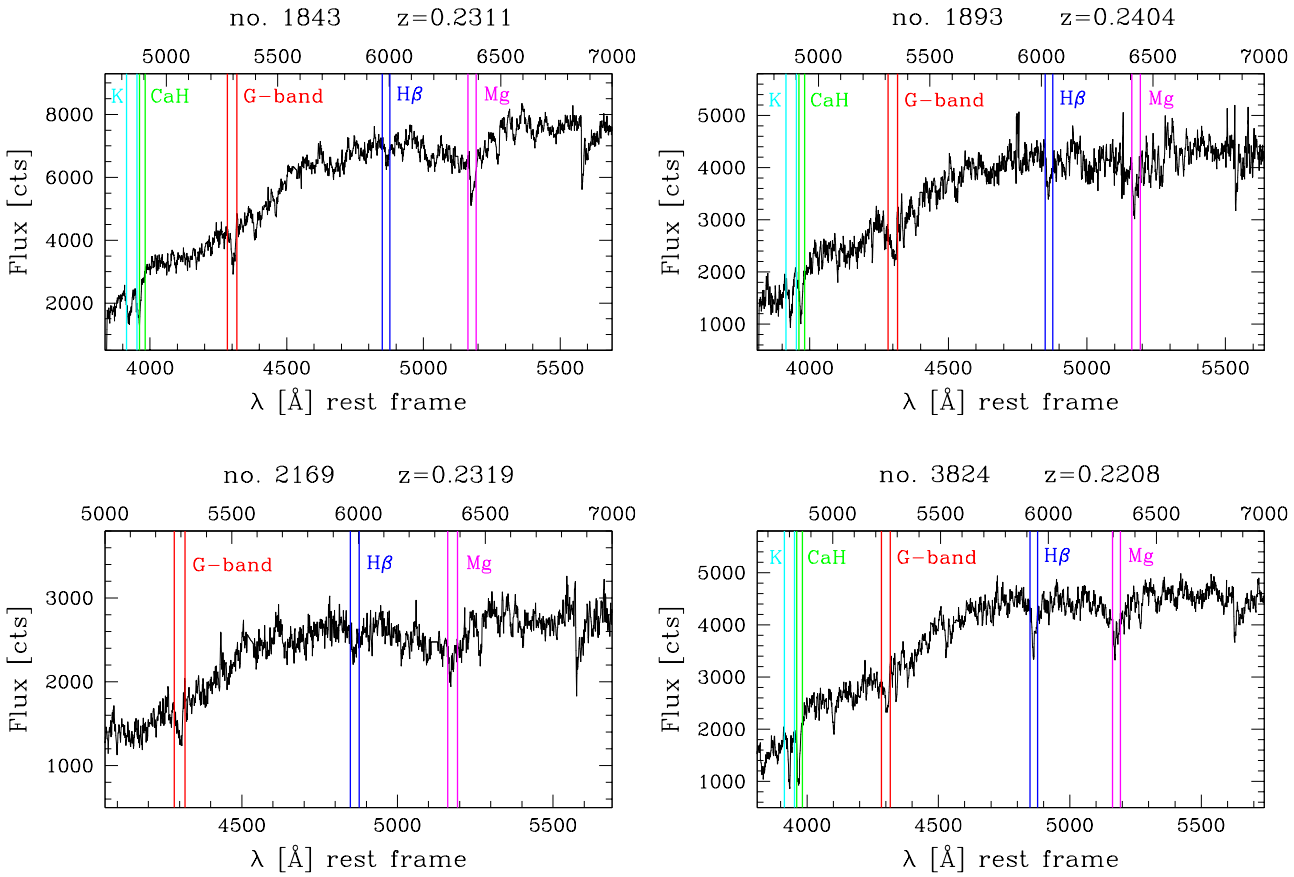

Figure 2: Spectra (not flux-calibrated) of early–type galaxies with determined redshift. The lower x-axis represents the rest frame wavelengths, the upper one the observed wavelengths (both in Å). The ordinate gives the flux in counts (1 ADU=1.1 e^{-1}). Prominent absorption features are marked.

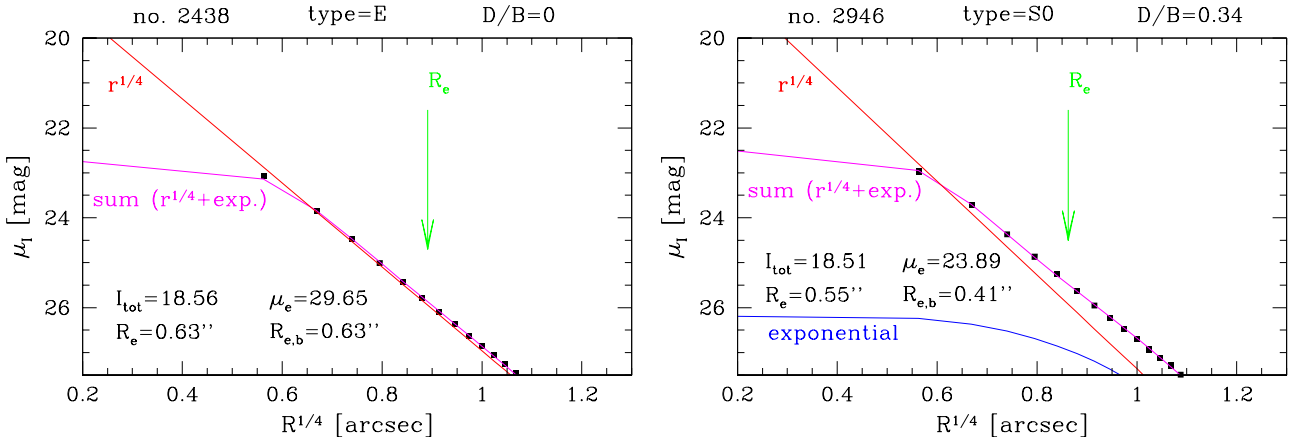

Figure 3: I_{814} Surface Brightness Profiles of two objects # 2438 (E) and # 2946 (S0). The total I_{814} magnitude (extinction A_{F814W} corrected) is plotted against the radius $R^{1/4}$ (in arcsec). Filled squares show the observed profile, the solid line is the best model for a combination of bulge and disk components (magenta), also splitted into the two separate components, a $r^{1/4}$-law (de Vaucouleurs law) (red) and a disk component fit (exponential law) (blue). The arrow indicates the position of the effective radius R_e. Various structural parameters are shown (see text for details). Typical residuals $\Delta\mu_I$ between the observed profile and the fit as a function of $R^{1/4}$ are in the order of $0.01 \leq \Delta\mu_I \leq 0.10$ (see Fritz et al. 2003a).

4 Results

4.1 HST Photometry

The surface brightness models for our galaxies were constructed using our F814W image. As pointed out by Ziegler et al. (1999), an exposure time of ~ 10 ksec is deep enough to determine structural parameters down to $m_B \sim 23$ mag.

4.1.1 Structual Parameter Analysis

Structural properties were determined by fitting the surface brightness profiles in the HST F814W images with an $r^{1/4}$ and an exponential law profile, both separately and in combination (Saglia et al. 1997). For the bulge profile a special form of the Sérsic profile (Sérsic 1968), the classical de Vaucouleurs profile ($r^{1/4}$-law), in the following form was applied:

$$\mu(R) = \mu_e \exp\{-7.67\,[(R/R_e)^{1/4} - 1]\} \quad (2)$$

$\mu(R)$ is the surface brightness at R along the semimajor axis and μ_e is the effective surface brightness. The disk profile is well represented by an exponential law, defined as:

$$\mu(R) = \mu_0 \exp\{-(R/h)\} \quad (3)$$

where μ_0 is the (face-on) central surface brightness for the disk and h the exponential disk scale length. In total structural parameters could be determined for 14 galaxies out of 15 for which we also have obtained spectra. In Fig. 3 examples of the Surface Brightness Profile (SBP) fitting are shown. Values for the total magnitude I_{tot}, the effective surface brightness μ_e, the effective radius R_e and the effective radius of the bulge $R_{e,b}$, and the disk-to-bulge ratio D/B are listed.
The model for the elliptical (E) galaxy # 2438 is well represented by a de Vaucouleurs profile with no additional disk component. In the case of the lenticular (S0) galaxy # 2946 a combined model of an $r^{1/4}$-law and an additional disk component results in the best model profile. For the innermost regions ($R^{1/4} \lesssim 0.5$), the model is extrapolated to the calculated central surface brightness μ_0 of the galaxy. Therefore, both galaxies are well reproduced by a combination of a de Vaucouleurs profile and a profile for an underlying disk component. Further details as well as a discussion on the residuals $\Delta\mu_I$ between the observed profile and the modelled fit as a function of $R^{1/4}$ are presented elsewhere, see Fritz et al. (2003a).

4.2 The Fundamental Plane at Intermediate Redshift

In Fig. 4 the Fundamental Plane (FP) for A 2390 in rest frame Gunn r is illustrated. The figure also shows the FP for the local Coma sample of Jørgensen et al. (1996) and the intermediate redshift cluster of A 2218 by Ziegler et al. (2001) at $z = 0.18$.
An analysis of the morphologies of the HST sub-sample galaxies revealed that our sample splits nearly equally into elliptical and lenticular (S0) galaxies. Seven galaxies were classified as elliptical, six as lenticular and one as an early-type spiral (Sa). Both subsets, elliptical as well as lenticular galaxies, are uniformly distributed along the Fundamental Plane (see Fig. 4). If we compare our FP results to the sample of 115 Coma galaxies we find a mild luminosity evolution of $\overline{m}_r = 0.07 \pm 0.10$ mag (using the WMAP cosmology: $H_0 = 71$ km s^{-1} Mpc^{-1}, $\Omega_m = 0.3$, $\Omega_\Lambda = 0.7$) for the overall sample. This finding is in good agreement with the predictions of hierachical models of cluster formation (Kauffmann 1996).
One of our main goals is to investigate possible differences between ellipticals and lenticular galaxies. Combining our sample of galaxies in A 2390 with an analogous study of the cluster Abell 2218 by Ziegler et al. (2001), we investigate in total ~ 100 early-type galaxies, one of the

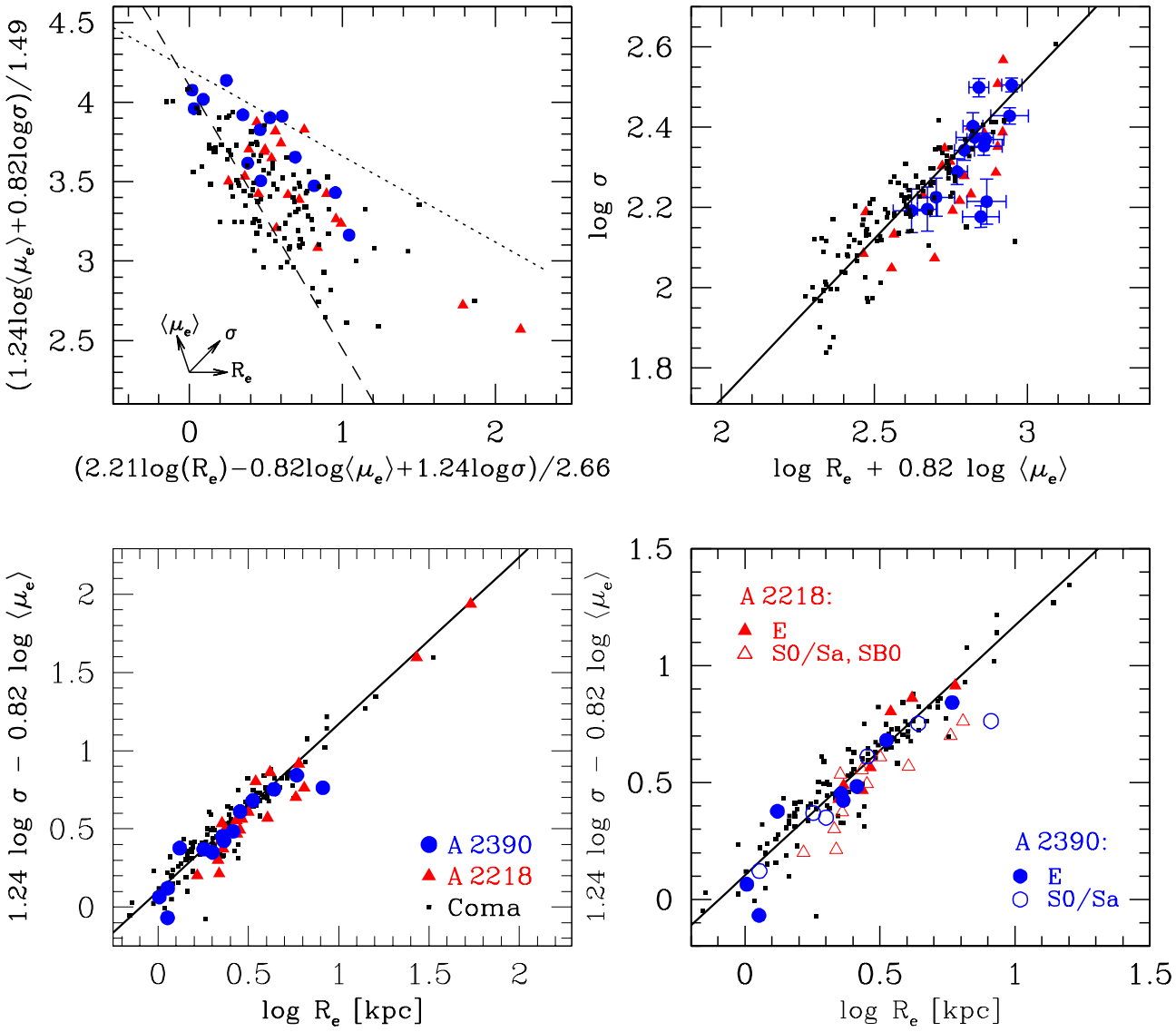

Figure 4: Fundamental Plane for the cluster A 2390 in rest frame Gunn r. Circles represent our A 2390 objects, triangles the early-type galaxies of A 2218 ($z = 0.18$), small squares the Coma galaxies of Jørgensen et al. (1996), respectively. *Upper panel, left:* Face on FP. The dotted line indicates the so-called exclusion zone for nearby galaxies (Bender et al. 1992) and the dashed line the luminosity limit for the completeness of the Coma sample $M_{r\,\mathrm{T}} = -20.75$ mag. *Upper panel, right:* FP edge-on, along the short axis. This panel shows the FP in the most natural view for a reliable error determination, with kinematics and photometric properties on different axes. As the errors of the photometric structual parameters are correlated, the combination of these errors enter the FP (see Fritz et al. 2003b for a detailed discussion). *Lower panel:* Edge-on FP. The solid line represents the bisector fit for the local Coma objects. On the left side a zoom of the edge-on FP with a separation into different morphologies, elliptical (E) and lenticular (S0) galaxies of the A 2390 and A 2218 galaxies is shown. We derive an FP evolution of $\overline{m}_r = 0.07 \pm 0.10$ mag compared to the local Coma sample (see text for details).

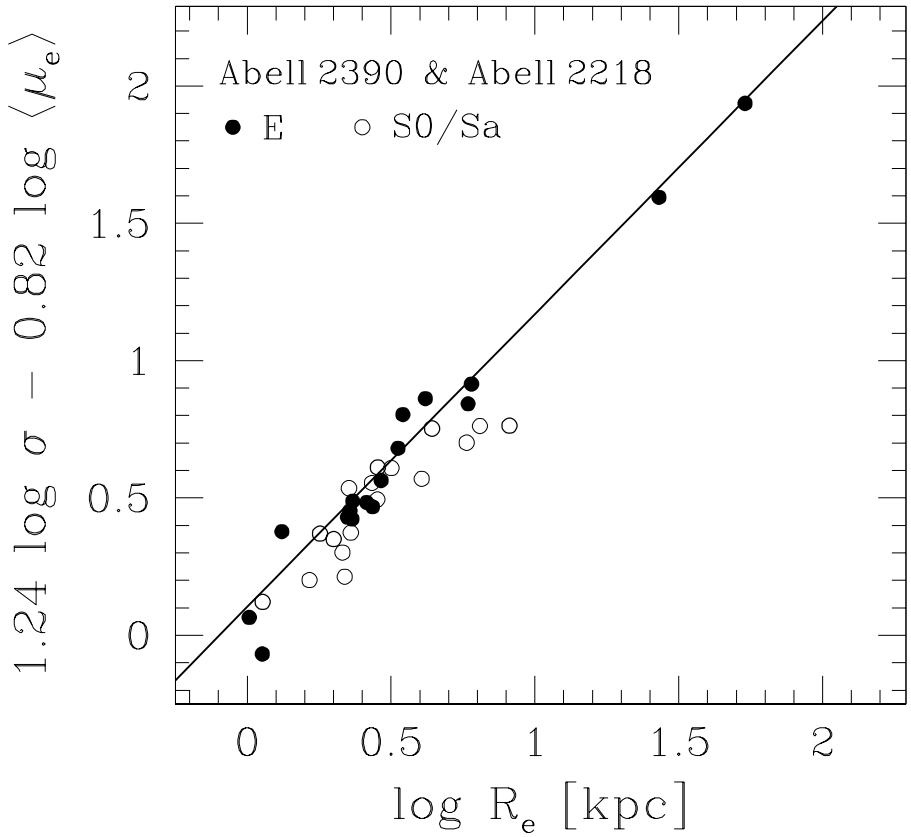

Figure 5: Edge-on view of the Fundamental Plane for A 2390 ($z = 0.23$) and A 2218 ($z = 0.18$) in rest frame Gunn r. The distant FP is compared with the FP for the local Coma sample (Jørgensen et al. 1996), indicated by the bisector fit. Lenticular galaxies seem to show a small zeropoint offset with respect to elliptical galaxies.

most extensive investigations at intermediate redshift ($z \sim 0.2$). A sub-sample with accurate structural parameter analysis provided by HST comprises 16 ellipticals, 11 S0, 3 SB0/a, 2 Sa and 1 Sab galaxy that enter the FP. Thus, with this large sample, possible radial and environmental dependences can be explored in detail for the galaxy properties from the cluster centre to the outskirts and for different sub-populations (E/S0, Sa bulges, E+A).
The Fundamental Plane for the intermediate clusters A 2390 ($z = 0.23$) and A 2218 ($z = 0.18$) in rest frame Gunn r is shown in Fig. 5. The distant FP for the clusters at intermediate redshift is compared with the FP for the local Coma sample (Jørgensen et al. 1996), indicated by the bisector fit. As the early-type cluster galaxies are equally distributed across the surface of the FP plane, an edge-on projection allows a reliable comparison of their stellar populations. Dividing the early-type galaxies of the two clusters into elliptical and lenticular galaxies, a slight offset change in the zeropoint of S0 galaxies arises with S0 galaxies lying predominantly below the ellipticals. Compared to the sample of 115 Coma galaxies we again deduce only a modest luminosity evolution. From the very small amount of luminosity evolution we conclude that at a look-back time of ~ 2.8 Gyrs most early-type galaxies of A 2390 consist of an old stellar population and that the bulk of the stars has formed at a much higher redshift of about $z_{\rm f} \geq 2$.

5 Discussion and Conclusions

In this paper we have presented results on the evolutionary status of the early-type galaxy population in the rich cluster Abell 2390 at $z = 0.23$.

The spectroscopic observations are based on Multi-Object-Spectroscopy with MOSCA at the 3.5 m Calar Alto telescope. Using the capabilities of the MOSCA spectrograph we have obtained a total of 63 high signal-to-noise early-type galaxy spectra. Within this large spectroscopic sample we have investigated 51 members of the A 2390 early-type galaxy population, both over a broad range in luminosity ($-19.3 \geq M_B \geq -22.3$) and a wide field of view of $10' \times 10'$. In addition, deep UBi ground-based imaging with the 5.1 m Hale telescope and HST photometry in the F555W and F814W filter are available, providing the possibility to construct the Faber-Jackson and Mg-σ relation for a large sample of early-type galaxies.

Structural properties of the HST sub-sample were analysed by combining an $r^{1/4}$ and an exponential law profile for accurate modelling of surface brightness profiles of the galaxies. Results on structual parameters provide the opportunity to establish the Fundamental Plane of the cluster galaxies at $z \sim 0.2$.

Elliptical and lenticular galaxies are both uniformly distributed across the surface of the Fundamental Plane. There maybe a hint that lenticular galaxies populate more the outskirts of the clusters, located slightly below the FP as seen in the edge-on projection of the FP. From the Fundamental Plane for A 2390 in rest frame Gunn r we deduce a modest luminosity evolution of $\overline{m}_r = 0.07 \pm 0.10$ mag for the overall sample compared to a local sample of 115 Coma galaxies (WMAP cosmology: $H_0 = 71$ km s^{-1} Mpc^{-1}, $\Omega_m = 0.3$, $\Omega_\Lambda = 0.7$). Thus, we conclude that the cluster A 2390 is populated by early-type galaxies consisting of old stellar populations and that the majority of the stars must have generated at a much higher formation epoch with a formation redshift of about $z_f \geq 2$. This is in agreement with the predictions of the hierarchical merging scenario for rich clusters.

Currently we are exploring the evolution of the galaxies in age, metallicity and abundance ratios by analysing absorption line strengths (e.g., Balmer lines, CN_1, Mg_b, Fe-indices) to compare them with stellar population models by Thomas et al. (2003). In addition, results from the two rich clusters will be set in contrast to ten poor low-L_X clusters at $z \sim 0.25$ to probe possible evironmental dependences of early-type galaxy evolution.

Acknowledgements:
AF is deeply grateful to Santos Pedraz for given the possibility to present results on this investigation. We thank A. Böhm for valuable discussions and comments on the article. This work is based on observations collected at the German–Spanish Astronomical Center, Calar Alto (CAHA), operated by the Max–Planck–Institut für Astronomie, Heidelberg, jointly with the Spanish National Commission for Astronomy, No. S99-3.5-048 and H00-3.5-028. The authors would like to thank the Calar Alto staff for efficient observational support. AF and BLZ acknowledge financial support by the Volkswagen Foundation (I/76 520) and the Deutsche Forschungsgemeinschaft (DFG) (ZI 663/1-1, ZI 663/2-1).

References

Bender, R. 1990, A&A, 229, 441
Bender, R., Burstein, D., Faber, S. M. 1992, ApJ, 399, 462
Bender, R., Burstein, D., Faber, S. M. 1993, ApJ, 411, 153
Bertin, E., Arnouts, S. 1996, A&AS, 117, 393
Caon, N., Capaccioli, M., D'Onofrio, M. 1993, MNRAS, 265, 1013
Djorgovski, S., Davis, M. 1987, ApJ, 313, 59

Dressler et al. 1987, ApJ, 313, 42
Faber, S. M., Jackson, R. E. 1976, ApJ, 204, 668
Fritz, A., Ziegler, B. L., Bower, R. G., Smail, I., Davies, R. L. 2003a, in *"Carnegie Observatories Astrophysics Series, Vol. 3: Clusters of Galaxies: Probes of Cosmological Structure and Galaxy Evolution"*, eds. J. S. Mulchaey, A. Dressler, and A. Oemler, in press, (Pasadena: Carnegie Observatories, http://www.ociw.edu/ociw/symposia/series/symposium3/proceedings.html).
Fritz, A., Ziegler, B. L., Bower, R. G., Smail, I., Davies, R. L. 2003b, MNRAS, in prep.
Graham, A., Lauer, T. R., Colless, M., Postman, M. 1996, ApJ, 465, 534
Guzmán, R., Lucey, J. R., & Bower, R. G. 1993, MNRAS, 265, 731
Jørgensen, I., Franx, M., Kjærgaard, P. 1996, MNRAS, 280, 167
Kauffmann, G. 1996, MNRAS, 281, 487
Kormendy, J. 1977, ApJ, 218, 333
Saglia, R. P., Bertschinger, E., Baggley, G. et al. 1997, ApJS, 109, 79
Sérsic, J. L. 1968, Atlas de galaxias australes (Cordoba, Argentina: Observatorio Astronomico)
Thomas, D., Maraston, C., Bender, R. 2003, MNRAS, 339, 897
Ziegler, B. L., Saglia, R. P., Bender, R., Belloni, P., Greggio, L., Seitz, S. 1999, A&A, 346, 13
Ziegler, B. L., Bower, R. G., Smail, I., Davies, R. L., Lee, D. 2001, MNRAS, 325, 1571